Prostate Cancer: Sextant Localization at MR Imaging and MR Spectroscopic Imaging before Prostatectomy—Results of ACRIN Prospective Multi-institutional Clinicopathologic Study[1]

Jeffrey C. Weinreb, MD
Jeffrey D. Blume, PhD
Fergus V. Coakley, MD
Thomas M. Wheeler, MD
Jean B. Cormack, PhD
Christopher K. Sotto, BS
Haesun Cho, MD
Akira Kawashima, MD, PhD
Clare M. Tempany-Afdhal, MD
Katarzyna J. Macura, MD, PhD
Mark Rosen, MD, PhD
Scott R. Gerst, MD
John Kurhanewicz, PhD

Purpose: To determine the incremental benefit of combined endorectal magnetic resonance (MR) imaging and MR spectroscopic imaging, as compared with endorectal MR imaging alone, for sextant localization of peripheral zone (PZ) prostate cancer.

Materials and Methods: This prospective multicenter study, conducted by the American College of Radiology Imaging Network (ACRIN) from February 2004 to June 2005, was institutional review board approved and HIPAA compliant. Research associates were required to follow consent guidelines approved by the Office for Human Research Protection and established by the institutional review boards. One hundred thirty-four patients with biopsy-proved prostate adenocarcinoma and scheduled to undergo radical prostatectomy were recruited at seven institutions. T1-weighted, T2-weighted, and spectroscopic MR sequences were performed at 1.5 T by using a pelvic phased-array coil in combination with an endorectal coil. Eight readers independently rated the likelihood of the presence of PZ cancer in each sextant by using a five-point scale—first on MR images alone and later on combined MR–MR spectroscopic images. Areas under the receiver operating characteristic curve (AUCs) were calculated with sextant as the unit of analysis. The presence or absence of cancer at centralized histopathologic evaluation of prostate specimens was the reference standard. Reader-specific receiver operating characteristic curves for values obtained with MR imaging alone and with combined MR imaging–MR spectroscopic imaging were developed. The AUCs were estimated by using Mann-Whitney statistics and appropriate 95% confidence intervals.

Results: Complete data were available for 110 patients (mean age, 58 years; range, 45–72 years). MR imaging alone and combined MR imaging–MR spectroscopic imaging had similar accuracy in PZ cancer localization (AUC, 0.60 vs 0.58, respectively; $P > .05$). AUCs for individual readers were 0.57–0.63 for MR imaging alone and 0.54–0.61 for combined MR imaging–MR spectroscopic imaging.

Conclusion: In patients who undergo radical prostatectomy, the accuracy of combined 1.5-T endorectal MR imaging–MR spectroscopic imaging for sextant localization of PZ prostate cancer is equal to that of MR imaging alone.

Supplemental material: *http://radiology.rsnajnls.org/cgi/content/full/251/1/122/DC1*

[1] From the Department of Radiology, Yale University School of Medicine, 333 Cedar St, PO Box 208042, New Haven, CT 06520 (J.C.W.); Center for Statistical Sciences, Brown University, Providence, RI (J.D.B., J.B.C.); Department of Radiology, University of California, San Francisco, San Francisco, Calif (F.V.C., C.K.S., J.K.); Department of Pathology, Baylor College of Medicine, Houston, Tex (T.M.W.); Department of Radiology, University of Texas M. D. Anderson Cancer Center, Houston, Tex (H.C.); Department of Radiology, Mayo Clinic, Rochester, Minn (A.K.); Department of Radiology, Brigham & Women's Hospital, Boston, Mass (C.M.T.); The Russell H. Morgan Department of Radiology and Radiological Science, Johns Hopkins University, Baltimore, Md (K.J.M.); Department of Radiology, University of Pennsylvania, Philadelphia, Pa (M.R.); and Department of Radiology, Memorial Sloan Kettering Cancer Center, New York, NY (S.R.G.). From the 2006 RSNA Annual Meeting. Received March 1, 2008; revision requested May 29; revision received October 7; accepted October 17; final version accepted November 6. **Address correspondence to** J.C.W. (e-mail: *jeffrey.weinreb@yale.edu*).

Radiology

Prostate cancer is the most common noncutaneous cancer and the second most common cause of cancer-related deaths in American men. In 2007, an estimated 218 890 new cases of prostate cancer were diagnosed and more than 27 000 men died of the disease (1). Additional indicators, including disability-adjusted life-years, estimated costs based on the Surveillance Epidemiology and End Results Program of the National Cancer Institute, and Medicare expenditures, illuminate the heavy burden that prostate cancer places on society (2,3). However, while the lifetime risk of receiving a diagnosis of prostate cancer is 16%, the lifetime risk of dying from prostate cancer is only 3% (4). The management of early-stage prostate cancer is controversial because patients whose disease is indolent and incidental cannot be reliably distinguished from those whose disease is progressive and life threatening. Traditional methods of prostate cancer evaluation involving digital rectal examination, transrectal ultrasonography (US), sextant biopsy, and serum prostate-specific antigen assay generally enable one to predict the behavior of very indolent or aggressive cancers only. Most patients have disease that falls between these extremes, for which these techniques—used alone or together—have limited diagnostic accuracy (5–10).

Given these limitations, investigators have studied the value of endorectal magnetic resonance (MR) imaging for assessing the local extent of prostate cancer and observed good results (11,12). The results of several studies also have indicated that MR spectroscopic imaging yields additional useful information based on the metabolic changes associated with the disease (13–15). As promising as these results may seem, there are only a small number of facilities worldwide that have staffs with substantial experience and expertise in MR spectroscopic imaging of the prostate and even fewer facilities where diagnostic accuracy studies to characterize the "discovery" and early "diffusion" stages in the application of emerging diagnostic methods have been performed (16). To our knowledge, scientifically rigorous trials with comparable quality and results across multiple institutions have not been conducted previously. Because of concerns about technical consistency and interobserver variability, the undertaking of such multi-institutional studies is essential if combined endorectal MR imaging–MR spectroscopic imaging of the prostate is to achieve widespread acceptance and use. Therefore, the American College of Radiology Imaging Network (ACRIN) undertook a prospective multi-institutional study to determine the incremental benefit of using combined endorectal MR imaging–MR spectroscopic imaging, as compared with endorectal MR imaging alone, for the sextant localization of peripheral zone (PZ) prostate cancer.

Advance in Knowledge

- In patients who undergo radical prostatectomy, the accuracy of combined endorectal MR imaging–MR spectroscopic imaging at 1.5 T for sextant localization of peripheral zone prostate cancer is equal to that of MR imaging alone.

Materials and Methods

The study was approved by the Cancer Therapy Evaluation Program of the National Cancer Institute and the institutional review boards of ACRIN and seven participating sites (University of California, San Francisco, University of Texas M. D. Anderson Cancer Center, Mayo Clinic, Brigham & Women's Hospital, Johns Hopkins Medical Institutions, University of Pennsylvania Medical Center, and Memorial Sloan Kettering Cancer Center). The study was also compliant with Health Insurance Portability and Accountability Act guidelines. Research associates were required to follow patient consent guidelines approved by the Office for Human Research Protection and established by the institutional review boards of the participating institutions.

The authors had control of the data and information submitted for publication. Authors who were not consultants for Medrad (Pittsburgh, Pa) or GE Healthcare (Waukesha, Wis) had control over the inclusion of any data and information that might have represented a conflict of interest for the author who was a consultant for one of these companies (J.K.). One author (J.K.) received royalties from GE Healthcare when the 1.5-T prostate MR imaging–MR spectroscopic imaging package described herein was released for commercial use and has received grant funding from GE Healthcare for the development of a 3.0-T MR imaging–MR spectroscopic imaging package.

Implication for Patient Care

- The addition of MR spectroscopic imaging to MR imaging at 1.5 T does not improve the ability to localize cancer within a sextant of the prostate.

Patient Inclusion and Exclusion Criteria

This prospective multi-institutional study was conducted by the ACRIN. Patients with biopsy-confirmed prostate adenocarcinoma who were scheduled for rad-

Published online before print
10.1148/radiol.2511080409

Radiology 2009; 251:122–133

Abbreviations:
ACRIN = American College of Radiology Imaging Network
AUC = area under receiver operating characteristic curve
PZ = peripheral zone

Author contributions:
Guarantor of integrity of entire study, J.C.W.; study concepts/study design or data acquisition or data analysis/interpretation, all authors; manuscript drafting or manuscript revision for important intellectual content, all authors; manuscript final version approval, all authors; literature research, J.C.W., T.M.W.; clinical studies, J.C.W., F.V.C., C.K.S., H.C., A.K., C.M.T., K.J.M., M.R., J.K.; experimental studies, J.C.W., T.M.W., J.K.; statistical analysis, J.C.W., J.D.B., J.B.C.; and manuscript editing, J.C.W., J.D.B., F.V.C., T.M.W., J.B.C., H.C., A.K., C.M.T., K.J.M., M.R., J.K.

Funding:
This research was supported by National Cancer Institute (grants U01 CA079778, U01 CA080098).

See Materials and Methods for pertinent disclosures.

ical prostatectomy were enrolled and underwent endorectal MR imaging and MR spectroscopic imaging from February 2004 to June 2005. Patient inclusion criteria were *(a)* biopsy-proved adenocarcinoma of the prostate with written documentation that radical prostatectomy at the participating site was anticipated within 6 months after the MR examination; *(b)* an interval of at least 6 weeks between diagnostic biopsy and the protocol MR examination; *(c)* radical prostatectomy performed within 6 months after the MR examination at the participating institution, with submission of histopathologic specimens for analysis; and *(d)* study-specific informed consent signed before study enrollment.

Subject exclusion criteria were *(a)* inability to give valid informed consent, whether because of age, a general medical or psychiatric condition, or a physiologic condition unrelated to the presence of prostate cancer; *(b)* unwillingness or inability to undergo MR imaging and MR spectroscopic imaging, including that due to contraindications to MR imaging; *(c)* contraindications to or inability to tolerate endorectal coil insertion—for example, before abdominoperineal resection of the rectum; *(d)* allergy to latex (present in endorectal coil); *(e)* surgery or other therapy that might alter the morphology or metabolism of the prostate before radical prostatectomy, including cryosurgery, transurethral prostate resection, pelvic radiation therapy, androgen deprivation therapy, use of PC Spes (Botanic Lab, Brea, Calif) (an alternative medicinal agent with hormonal activity), or bacillus Calmette-Guérin vaccine for bladder cancer; and/or *(f)* metallic hip implant or any other metallic implant or device that might distort the local magnetic field homogeneity and compromise the quality of the MR spectroscopic imaging examination.

Patient Recruitment

Patients were recruited from the urology clinics of the seven participating institutions. Subject eligibility was first assessed by the participating urologists, who then contacted the institutional ACRIN research associate so that he or she could further discuss the study with the patient. Patients were enrolled before they underwent surgery and after they signed a study-specific informed consent form. A target study population of 134 patients was established on the basis of initial power calculations (described in Statistical Analyses).

The target study population of 134 patients (mean age, 58 years; range, 39–74 years) was recruited. Twenty-four patients were subsequently deemed ineligible because *(a)* the interval between biopsy and MR imaging was less than 6 weeks ($n = 3$), *(b)* they had undergone hormonal therapy ($n = 1$), *(c)* they previously had undergone transurethral prostate resection ($n = 1$), *(d)* they declined to undergo MR imaging after initial enrollment ($n = 1$), *(e)* the MR examination could not be completed owing to anxiety or claustrophobia ($n = 6$), *(f)* spectroscopic imaging was not performed as part of the MR examination ($n = 1$), *(g)* surgery was not performed within 6 months after the MR examination ($n = 5$), *(h)* histopathologic specimens were not submitted for central review ($n = 4$), and/or *(i)* the MR data were of poor quality ($n = 2$).

Participating Site Selection Criteria

Seven academic medical centers in the United States that met the following criteria participated in the study: *(a)* They submitted a protocol-specific application to ACRIN headquarters. *(b)* They provided a documented record of having performed at least 50 radical prostatectomies per year. *(c)* A 1.5-T MR unit with endorectal MR imaging and MR spectroscopic imaging capability was installed at their facility. Only GE Healthcare units were qualified since at the time the study was developed and initiated this company was the only vendor with Food and Drug Administration–approved capability for the complete data acquisition and analysis protocol described herein. In addition, in this early period of technology diffusion, it was desirable to ensure technical uniformity—a goal best accomplished by using equipment from a single vendor. *(d)* The participating site pathologist supplied a written commitment to provide appropriate histopathologic specimens—including step-section or whole-mount specimens of the entire prostate and lower seminal vesicles—for central analysis. *(e)* The designated radiologist, urologist, and pathologist at the given institution provided signed documentation of his or her willingness and commitment to participate in the study. *(f)* A designated research associate and MR technologist participated in the investigation.

MR Imaging and MR Spectroscopic Imaging Techniques

The patients were instructed to self-administer a commercially available nonprescription sodium biphosphate–sodium phosphate enema (Fleet Enema; C. B. Fleet, Lynchburg, Va) on the day of the MR examination to clean the rectum and prevent degradation of the MR spectroscopic images from fecal residue.

All MR examinations were performed by using 1.5-T whole-body GE Healthcare MR units. Patients were imaged in the supine position with a pelvic phased-array coil that was interfaced with a disposable expandable endorectal coil (eCoil Imaging System; Medrad) via an ATD III connector (GE Healthcare). Both coils are receive-only devices. The endorectal coil was positioned to lie immediately posterior to the prostate, the balloon was filled with air, and the coil was centered on the prostate in the axial plane. Sagittal rapid acquisition with relaxation enhancement localizer images were used to check the position of the coil, which was adjusted as necessary. The technical parameters used to perform the MR imaging and MR spectroscopic pulse sequences are summarized in Table 1.

Three-dimensional MR spectroscopic images of the prostate were acquired by using a commercial version of the point-resolved spectroscopy sequence (PROSE; GE Healthcare). A detailed description of this sequence is provided in Appendix E1 (*http://radiology.rsnajnls.org/cgi/content/full/251/1/122/DC1*) (17–20).

Spectral data were processed at an Advantage workstation (GE Healthcare), aligned with the corresponding MR images by using voxel-shifting and baseline phase–correcting tools available with the point-resolved spectroscopy sequence package, and archived as an array of spectral data (including automated estimates of the choline plus creatine–to citrate ratio and the choline-to-creatine ratio) with the corresponding MR images in Digital Imaging and Communications in Medicine format. Peak area ratios were calculated by means of integration of the metabolite peak over a fixed frequency range defined in a peak file containing peak positions and widths.

Site Certification and Quality Assurance

Although personnel at all of the sites had experience in endorectal MR imaging of the prostate, endorectal MR spectroscopic imaging of the prostate was being performed routinely at only two sites prior to commencement of the study. Accordingly, site certification and quality assurance were integral to the study protocol and included the following features:

Prior to the start of the trial, all participating sites received a quality assurance prostate phantom with the PROSE software. Technologists at all participating sites were trained in acquiring prostate imaging and spectral data from the phantom and nonstudy subjects. Before study patients were enrolled, each site had to demonstrate proficiency in acquiring acceptable-quality prostate images and spectra from the phantom and three test subjects who were not included as patients in this study. Data quality was assessed by an expert panel of two individuals from the group of study investigators: a radiologist (F.V.C.) and a spectroscopist (J.K.) with more than 10 years experience in endorectal MR imaging and MR spectroscopic imaging of the prostate. Each site received feedback regarding the test cases rated as unacceptable and had to provide additional acceptable data sets before enrolling the first study patient.

Before the start of the trial, the designated research associate and radiologist from each participating site attended an intensive 1-day workshop that entailed didactic lectures and hands-on training in performing endorectal MR imaging and MR spectroscopic imaging of the prostate and interpreting the resultant data. The workshop was organized by the Department of Radiology of the University of California, San Francisco. Designated spectroscopists and MR physicists from some of the sites also attended this workshop.

During the course of the trial, investigators from all sites performed quality assurance phantom studies within 1 week before the patient examinations to ensure that the MR unit was functioning properly for the acquisition of reproducible data. This was accomplished by using the GE Healthcare brain spectroscopy phantom, which yielded data that, compared with the quality assurance prostate phantom data, allowed a more straightforward evaluation of important technical parameters, including shim value, spectrometer gain, water line width, and metabolite signal-to-noise ratios. A single-voxel spectroscopy package (PROSE) with body excitation and 5-inch surface coil receive capability was used to ac-

Table 1

Parameters for MR Imaging and MR Spectroscopy at 1.5 T

Parameter	Axial T1-weighted Spin Echo or Fast Spin Echo*	Axial High-Spatial-Resolution Fast Spin Echo†	Coronal High-Spatial-Resolution Fast Spin Echo†	Spectroscopic Spatial 3D‡
Coil	Torso phased-array, endorectal	Torso phased-array, endorectal	Torso phased-array, endorectal	Endorectal only
Anatomic coverage	Aortic bifurcation to symphysis pubis	Prostate and seminal vesicles	Prostate and seminal vesicles	Prostate, (determined from axial T2-weighted images)
TR msec/TE msec§	600–700/12	4000–6000/90–120	4000-6000/90–120	1000/130
Section thickness (mm)‖	4–6 (0–1)	3 (0–1)	3 (0–1)	7 (0)
Field of view (mm)	200–320	100–140	100–140	110 × 55 × 55
Frequency direction	Transverse	Anteroposterior	Anteroposterior or superoinferior	. . .
Matrix	256 × 192	256 × 192	256 × 192	16 × 8 × 8
No. of signals acquired	One	Three to four	Three to four	One
Echo train length	. . .	Eight to sixteen	Eight to sixteen	. . .
Spectral width (Hz)	. . .	. . .	. . .	1000
Points	. . .	. . .	. . .	512
No. of signals per phase-encoding step	. . .	. . .	. . .	One

* For axial T1-weighted spin-echo or fast spin-echo imaging, a transverse frequency was applied to prevent endorectal coil motion–induced artifacts from obscuring the pelvic nodes.

† The high-spatial-resolution fast spin-echo sequences involved thin-section acquisition. An anteroposterior frequency was applied to prevent endorectal coil motion–induced artifacts from obscuring the prostate gland.

‡ For spectroscopic spatial three-dimensional (3D) imaging, shim water resonance to 12 Hz or lower and a spatial resolution of .3 cm^3 were applied.

§ TE = echo time, TR = repetition time.

‖ Numbers in parentheses are the intersection gap, expressed in millimeters.

quire spectra from the spherical brain spectroscopy phantom. The spectroscopy package included a standard quality assurance protocol, which for a given fixed set of acquisition parameters yielded robust metabolite peak signal-to-noise ratios that could be checked across sites.

MR Image and MR Spectroscopic Image Interpretation

Eight readers independently interpreted all images. These readers were one designated reader at each institution (F.V.C., H.C., A.K., C.M.T., K.J.M., M.R., S.R.G.) and the principal study investigator (J.C.W.), whose home institution was not a participating site. Two readers had less than 2 years experience performing endorectal MR imaging and interpreting the resultant images, two readers had 2–5 years experience, three readers had 6–10 years experience, and one reader had more than 10 years experience. Each reader analyzed the cases from his or her own institution and all the cases from the other participating sites. For each case, the MR image was read first and the combined conventional MR–MR spectroscopic image was read immediately thereafter. The readers were aware that the patient had biopsy-proved prostate cancer but unaware of all other clinical, laboratory, and histopathologic data. To prevent any untoward clinical consequence of this lack of awareness, the case images and the formal clinical report, which was issued by a different radiologist who was aware of all relevant clinical findings, were read separately.

Readers rated the likelihood of PZ cancer presence in each sextant by using a five-point scale, with a score of 1 indicating PZ cancer was definitely not present and a score of 5 indicating that it definitely was present. They rated the cancer likelihood first by using the MR images alone and later by using the combined MR–MR spectroscopic images. The readers recorded the maximal axial diameter of the largest focus suspected of being malignant in each sextant and noted the location of these foci on a diagrammatic representation of the prostate.

With use of an MR spectroscopic imaging overlay sheet and preestablished criteria for the probability of malignancy based on the choline plus creatine–to citrate ratio and the choline-to-creatine ratio, the location and size of areas suspicious for cancer in the PZ of the prostate were determined and the type and total number of abnormal voxels were recorded for each lesion depicted at MR spectroscopic imaging. The readers evaluated the degree of concordance between the MR imaging and combined MR imaging–MR spectroscopic imaging findings by noting the subset of abnormal MR spectroscopic imaging voxels that were concordant with the abnormal MR findings (ie, voxels that demonstrated reduced signal intensity in at least 50% of their extent at T2-weighted imaging). In general, cancer was characterized morphologically as an ovoid masslike or crescentic subcapsular focus of reduced signal intensity on T2-weighted images and was characterized metabolically by the presence of one or more voxels with suspicious metabolism—that is, with the choline peak elevated or the citrate peak reduced such that these two peaks were of similar height or the choline peak was higher than the citrate peak. When there was discordance between the MR imaging signal intensity and MR spectral findings, the reader was instructed to give an intermediate score (ie, 3); however, on the basis of the readers' assessment and associated findings, other scores were not precluded.

Although metabolic ratios and quantitative values of the spectra for the metabolites of interest were recorded, they were not the focus of this study and were not used because there were no fixed quantitative criteria for prostate cancer identification. (This issue is further addressed in the Discussion.)

Because there is no anatomic landmark that reproducibly indicates the boundaries between the base, middle region, and apex of the prostate, and for consistency in defining sextants among all the readers, the reader at the institution where each examination was performed first determined the anatomic location for each oblique axial T2-weighted and spectroscopic image section. To ensure anatomic consistency, each subsequent reader was then required to use the anatomic section assignments of the host primary institution for that case. When an odd number of voxels were present in the left-right dimension and the central voxel straddled the midline, this voxel was assigned to the right side by the reader at the institution where the data were acquired. No information other than this was provided to the off-site readers. The central part of the gland was not evaluated.

Histopathologic Reference Standard

Radical prostatectomy tissue specimens were coated with standard marking ink and fixed in buffered formaldehyde. The weight of the specimen, with the seminal vesicles excluded, was recorded after fixation. The fixed specimen was sliced, and two sets of slides were prepared: one set for routine analysis at the local institution and one set for central submission to the ACRIN. The slides were prepared as either whole-mount step sections or standard blocks according to the equipment and personnel expertise at the participating institution. To prepare whole-mount step sections, axial slices through the entire gland were obtained at 3–4-mm intervals in a plane perpendicular to the long axis of the prostate. To prepare standard blocks, axial slices through the prostate and seminal vesicles were obtained at 3–4-mm intervals in a plane perpendicular to the long axis of the prostate and inserted into standard numbered blocks by using an established method that enables reconstruction of the prostate for tumor mapping, localization, and measurement (21).

All slides sent for centralized ACRIN review were analyzed by the study pathologist (T.M.W.). The study pathologist was provided with pathology reports from the participating institutions. The location, grade, and size of the tumor were recorded on a standardized schematic diagram of the prostate that corresponded to the MR schematic diagrams. All tumor foci were evaluated; this assessment included determining

whether the foci were in the central part of the gland or in the PZ. Whether the dominant tumor in each patient was in the central region or PZ was also noted. The tumor stage determined by using current American Joint Committee on Cancer criteria (22) was recorded. The interpretation provided by the study pathologist served as the histopathologic reference standard for all data analyses.

Data and Image Handling

Data were collected, managed, and analyzed by personnel from the ACRIN Biostatistics Center and the ACRIN Data Management Center. The Biostatistics Center is located at the Center for Statistical Sciences in Providence, RI. The Data Management Center is located at the Data Management Department of the American College of Radiology in Philadelphia, Pa (Appendix E1, *http://radiology.rsnajnls.org/cgi/content/full/251/1/122/DC1*).

Expert Panel Review

Reference-standard information, defined as the presence or absence of cancer in a prostate sextant, was critical to the statistical analysis. Use of the sextant definitions established by the radiologist at the participating site ensured that all readers were defining the sextants in the same fashion. However, there was no way to directly associate these imaging-based sextant definitions to the histopathologic reference standard. To address this issue, an expert panel was convened after the study was completed and all reader interpretations were received. The expert panel consisted of the principal investigator (J.C.W.), the co–principal investigator (F.V.C.), the study spectroscopic consultant (J.K.), and the project pathologist (T.M.W.). Oversight and support for this panel were provided by the study statistician (J.D.B.) and personnel from the ACRIN Biostatistics and Data Management Centers. The role of the expert panel was to determine whether cancer was present or absent in each sextant of the prostate by using the sextant definitions provided by the local radiologists and the histopathologic specimen data as the reference standards. Once the panel agreed on the correlation between the MR and histopathologic findings, the presence or absence of cancer in each sextant was recorded. For the sextants with cancer, the axial long- and short-axis measurements of the tumor were also noted. The histopathologic slides were digitized and viewed on a computer monitor alongside the MR images for 2 days at the ACRIN headquarters in Philadelphia. The MR images were correlated with the histopathologic specimens by using landmarks such as the urethra, ejaculatory ducts, nodules of benign prostrate hyperplasia, and obvious cancers.

The image quality of the entire three-dimensional MR imaging and MR spectroscopic imaging data sets was also assessed at this review. The quality of the MR images was rated as diagnostic or nondiagnostic by the principal investigator (J.C.W.) and the co–principal investigator (F.V.C.); they also recorded the presence or absence of postbiopsy hemorrhage on the T1-weighted images. Nondiagnostic images were those degraded by motion or other artifacts to the extent that the artifacts prevented the meaningful evaluation of tumor location. The study spectroscopic consultant (J.K.) scored the quality of the MR spectra by using a five-point scale, where a score of 5 indicated excellent spectral quality and a score of 1 indicated nondiagnostic quality (23). An MR spectroscopic image was considered to have excellent spectral quality (score of 5) when the signal-to-noise ratios of all metabolites were higher than 10, all metabolic resonances were well resolved, and there were no baseline distortions due to residual water or lipid. An MR spectroscopic image was considered to have good spectral quality (score of 4) when the signal-to-noise ratios of all metabolites were between 8 and 10, all metabolic resonances were reasonably well resolved, or there were minimal baseline distortions due to residual water or lipid. Spectroscopic images with lower signal-to-noise ratios were considered to be of fair spectral quality (score of 3), provided there was no lipid contamination. Spectroscopic images with substantial lipid contamination were considered to be of poor spectral quality (score of 2). Spectroscopic images in which lipid contamination or other artifacts prevented meaningful evaluation of the spectral signal were considered to be nondiagnostic (score of 1).

Statistical Analyses

The primary aim of this study was to determine whether using combined MR imaging–MR spectroscopic imaging, as compared with using MR imaging alone, improved the accuracy of detecting foci of PZ prostate cancer on a sextant-by-sextant basis. It was determined that a study sample of 134 patients and at least five readers would provide sufficient power to detect a difference between combined MR imaging–MR spectroscopic imaging with an accuracy of 0.73 and MR imaging alone with an accuracy of 0.65 (14) when a two-sided 5% level test with a positive sextant–to–negative sextant ratio of 1:2 was used and an inflation factor of 33% was used to account for cases with incomplete data sets—specifically, those with missing reference-standard findings and missing correlation of sextants (24). The methods of Obuchowski and McClish (25–28) were used for this computation.

For this study, the primary unit of analysis was the prostate sextant and the reference-standard finding was the presence or absence of cancer in the sextant at histopathologic analysis; these parameters were agreed on by members of the expert panel. The histopathologic volume of PZ cancer in each sextant *(V)* was calculated from the long- and short-axis diameters by using the formula $V = (4/3) \cdot \pi \cdot (D/2)^3$ (29), where D is the average of the long- and short-axis diameters. SAS, version 9.0 (SAS Institute, Cary, NC); Stata, version 9.0 (Stata, College Station, Tex); and S-PLUS, version 7.0 (Insightful, Seattle, Wash), statistical software was used for data processing and statistical analyses.

Initially, summary tables and simple frequencies were used to assess the data and check for outliers. As a first step in the analysis, we dichotomized

the results of all image readings to compute the sensitivity, specificity, and positive and negative predictive values for both MR imaging alone and combined MR imaging–MR spectroscopic imaging. To account for the trade off between sensitivity and specificity, the full range of assessments made on the five-point ordinal scale for likelihood of cancer was analyzed by using a receiver operating characteristic method. Specifically, reader-specific receiver operating characteristic curves for the values achieved with both MR imaging alone and combined MR imaging–MR spectroscopic imaging were developed, and the two areas under the receiver operating characteristic curves (AUCs) were estimated by using Mann-Whitney statistics with appropriate 95% confidence intervals. Before the diagnostic accuracy values of MR imaging alone and combined MR imaging–MR spectroscopic imaging were compared, 95% confidence intervals of the average AUCs for MR imaging alone and combined MR imaging–MR spectroscopic imaging across institutions were derived (25).

Parametric comparisons were also performed by using appropriately constructed analysis of variance models. Freely available software (*http://www.bio.ri.ccf.org/html/rocanalysis.html*) was used to perform this primary comparison. Nonparametric comparisons of average AUCs were made by using a *U* statistic approach that enabled us to account for the correlation between sextants and readers. With use of both the nonparametric and the parametric approaches, the correlation that resulted from imaging the patients with both techniques was taken into consideration. These analyses were also used to examine possible variations in diagnostic performance that were based on patient characteristics, reader characteristics, and other covariates with simple stratification.

A key design characteristic of this study was the forcing of readers to render a specific assessment for each sextant of the prostate. This characteristic enabled us to evaluate the primary parameter: the accuracy with which readers can locate or detect cancer in a sextant of the prostate once the sextant is defined. The choice of sextants was inconsequential for our analysis: The only requirement for generalizability was that the readers evaluate the identical images that were assigned to each sextant in the prostate. However, any approach that involves subdividing the prostate may be limited by the potential for "chance detections" (30). The rationale for performing the sextant-by-sextant analysis is described in Appendix E1 *(http://radiology.rsnajnls.org/cgi/content/full/251/1/122/DC1)*.

Results

Study Participants

The mean age for the final group of 110 study patients was 58 years (range, prostate-specific 45–72 years). The mean prostatie-specific antigen level was 5.9 ng/dL (range, 0.7–44.0 ng/dL). The mean interval between biopsy and MR imaging was 13 weeks (range, 6–55 weeks). The mean interval between MR imaging and surgery was 12 days (range, 0–158 days).

Histopathologic Analysis

In the final study group of 110 patients, prostatectomy tissue specimens were analyzed by using whole-mount step sections in 22 patients and by using standard blocks in 88. No PZ cancer was detected in three patients, one patient had cancer confined to the central part of the gland, and two patients had no detectable cancer in the prostate. Of the 107 patients with PZ cancer, 47 also had cancer in the central part of the gland, and in 11 of these patients, the cancer was dominant in the central region. The mean and median PZ tumor volumes in the 107 patients were 2.75 and 1.14 cm^3, respectively (range, 0.01–45.29 cm^3). The distribution of PZ tumor volumes is shown in Figure 1. The histopathologic tumor stages in the 107 patients with cancer in the surgical specimen were pT2 (organ confined) in 83 patients, pT3a (extracapsular extension) in 18, and pT3b (seminal vesicle invasion) in six; no patient had stage T4 disease. The median Gleason score was 7 (range, 3–9). Thirty-nine patients had palpable disease at digital rectal examination. In the final study population of 110 men, 393 of 660 analyzed sextants contained PZ cancer.

MR Image and MR Spectroscopic Image Quality

At expert panel review, the MR image quality of all 110 imaging studies was considered to be diagnostic. In 45 studies, postbiopsy hemorrhage was considered to be present. The distribution of MR spectral quality scores assigned by the study spectroscopic consultant at the time of expert panel review are shown in Table 2. Sixty-five studies

Figure 1

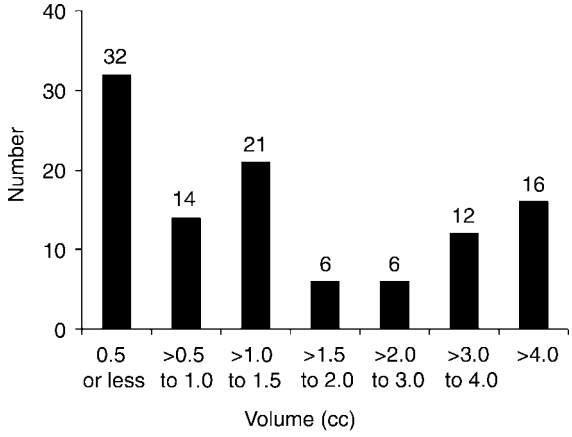

Figure 1: Graph shows distribution of histopathologic PZ tumor volumes. Numbers at top of bars are numbers of patients.

were assigned a good or excellent spectral quality score. Twenty-one studies were rated as poor, and six were rated as nondiagnostic. Sixty-nine (63%) of the 110 examinations were performed at three institutions and accounted for thirteen (48%) of all poor or nondiagnostic MR spectroscopic imaging studies. Twenty-three (21%) examinations were performed at two institutions and accounted for 12 (44%) of the poor or nondiagnostic MR spectroscopic imaging examinations.

Table 2

Distribution of MR Spectral Quality Scores Assigned per Patient

Institution	Spectral Quality Score					
	5	4	3	2	1	Total
A	3	6	5	5	0	19
B	1	3	2	6	2	14
C	3	9	4	3	1	20
D	0	4	0	1	0	5
E	6	5	1	1	0	13
F	1	3	1	2	2	9
G	7	14	5	3	1	30
Total	21	44	18	21	6	110

Note.—MR spectral quality scores were assigned per patient by the study spectroscopic consultant at the time of expert panel review.

Figure 2

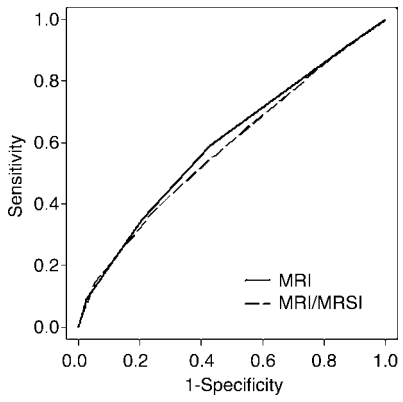

Figure 2: Receiver operating characteristic curves of MR imaging values versus combined MR imaging–MR spectroscopic imaging *(MRSI)* values for all readers.

MR Imaging and MR Imaging–MR Spectroscopic Imaging Tumor Localization

With eight independent readers, six sextants analyzed per patient, and 110 patients, the final analysis included 5280 sextants. MR imaging alone (AUC, 0.60) and combined MR imaging–MR spectroscopic imaging (AUC, 0.58) had similar accuracy in PZ cancer localization ($P = .09$) (Fig 2). The AUCs for individual readers are shown in Table 3 and ranged from 0.57 to 0.63 for MR imaging alone and from 0.54 to 0.61 for combined MR imaging–MR spectroscopic imaging (Fig 3).

Overall, there was no demonstrable incremental benefit from performing combined MR imaging–MR spectroscopic imaging rather than MR imaging alone, and most readers had similar AUCs for MR imaging alone and combined MR imaging–MR spectroscopic imaging. For two readers, however, the AUC for the combined examination was significantly lower ($P < .05$) (Table 3). In terms of sensitivity, both MR imaging alone and combined MR imaging–MR spectroscopic imaging performed significantly better in the detection of tumors greater than 10 mm in largest axial diameter and tumors with a volume greater than 0.5 cm^3. These results were not influenced by the spectroscopic imaging spectral score, Gleason score, presence of postbiopsy hemorrhage, or tumor palpability at rectal examination. These subgroup analyses are summarized in Appendix E1 *(http://radiology.rsnajnls.org/cgi/content/full/251/1/122/DC1)*.

Discussion

The results of this multi-institutional study indicate that MR imaging alone and combined MR imaging–MR spectroscopic imaging had similar modest accuracy in the sextant localization of PZ prostate cancer. However, they did not confirm our primary hypothesis that the addition of MR spectroscopic imaging to MR imaging would improve tumor localization. This hypothesis was based on prior single-institution study results, which indicated that the addition of MR spectroscopic imaging to MR imaging improves tumor localization (14,31), tumor volume estimation (15), tumor staging for less experienced readers (17), and tissue characterization (32,33). Given the preponderance of evidence that MR spectroscopic imaging adds value to MR imaging in the evaluation of prostate cancer, it is reasonable to ask why our study did not reveal this benefit. There are several possible reasons: First, our study population consisted of a contemporary series of North American patients who underwent radical prostatectomy. Such populations, in which diagnoses are being rendered during an era of widespread prostate-specific antigen testing, inevitably will include predominantly patients with low risk and small disease volume (typically clinical stage T1c). The mean prostate-specific antigen level in our study population (5.9

Table 3

AUCs for Sextant PZ Prostate Cancer Localization with MR Imaging Alone and Combined MR Imaging–MR Spectroscopic Imaging

Reader	MR Imaging	Combined MR Imaging–MR Spectroscopic Imaging	*P* Value
1	0.6028	0.5856	.2614
2	0.5723	0.5425	.2399
3	0.6264	0.5907	.0475
4	0.6054	0.5933	.5311
5	0.6163	0.6050	.6271
6	0.6092	0.5741	.0268
7	0.5863	0.5930	.7359
8	0.6099	0.6029	.6338
All Readers	0.6007	0.5844	.0892

ng/dL) was lower than the mean values reported in other studies—8.2 ng/dL (14,17), 8.0 ng/dL (31), 10.2 ng/dL (32), and 13.9 ng/dL (33)—and thus supports the view that our study population was skewed toward patients with low risk and low-volume disease despite a median Gleason score of 7.

Second, many of the tumors detected in our study were at or below the current spatial resolution of MR spectroscopic imaging. The MR spectroscopic imaging voxel size in this study was 0.34 cm^3. In the ideal scenario in which both the tumor and the voxel have the same geometric center, a spherical tumor must be at least 0.93 cm^3 to completely fill a 0.34-cm^3 voxel, and more than one-third of the tumors in our study population were below this size threshold.

Third, this study involved the distribution of a recently introduced technology—endorectal MR spectroscopic imaging—to multiple sites and readers with limited or no previous experience with it. The ACRIN's successful fulfillment of this study requirement is a nontrivial accomplishment, and it is noteworthy that imaging studies of generally good spectral quality were acquired at the sites despite the limited experience (involving a small number of test cases) of their personnel. Nevertheless, there were definite differences in the quality of the MR spectroscopic imaging data between the different participating institutions, two of which together contributed only 21% of the cases and accounted for 44% of the poor or nondiagnostic MR spectroscopic imaging examinations. Likewise, for six readers, the sextant localization of cancer was similar between MR imaging alone and combined MR imaging–MR spectroscopic imaging; however, two readers' diagnostic interpretations of the combined MR imaging–MR spectroscopic imaging data were less accurate. These results were not unexpected in the early stages during which this recently introduced diagnostic imaging tool was distributed. With increasing experience, the uniformity and quality of MR spectroscopic imaging data and the interpretation of combined MR imaging–MR spectroscopic imaging data are likely to improve.

It is instructive to compare our results with those of prior multi-institutional and large studies of prostate cancer imaging. An earlier multi-institutional study performed by the Radiology Diagnostic Oncology Group, which had many features similar to those of the ACRIN trial described herein, showed no difference in AUCs between MR imaging (0.67) and transrectal US (0.62) in the detection of extracapsular extension (34). The Radiology Diagnostic Oncology Group study data were published in 1990, the investigation did not involve the use of surface or endorectal coils but rather the use of MR technology and pulse sequences that are now obsolete, and the investigators did not explicitly describe the imaging criteria used to diagnose extracapsular extension. Furthermore, the investigators did not attempt to assess the capability for tumor localization.

Investigators in another multi-institutional trial found that using an endorectal coil in conjunction with standard body coils did not improve tumor staging accuracy (61% with body coils alone vs 57% with combined endorectal and body coils) (35). However, this study also involved the use of hardware and software that are now outdated. The study results did, however, show wide interreader variability. D'Amico et al (36) evaluated the role of MR imaging in predicting the time to prostate-specific antigen failure after radical prostatectomy in 1025 men. Patients in medium- and high-cancer-risk groups (based on stratification performed by using prostate-specific antigen level, Gleason score, stage at digital rectal examination, and percentage of biopsies with results positive for cancer) who had stage T3 disease at MR imaging had a significantly worse prognosis than did those with T2 disease at MR imaging. In the low-risk group (61% of the population), the distinction between T3 and T2 disease at imaging was not of prognostic importance. Overall, the results of these studies support the concept that MR imaging has limited accuracy, particularly when performed in patients with low cancer risk. Investigators in future trials of endorectal MR imaging and MR spectroscopic imaging will need to pay close attention to patient selection because the value of this technology may lie in its diagnostic performance in intermediate- and higher-risk groups.

Figure 3

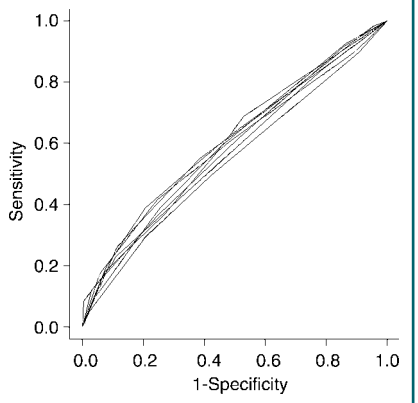

Figure 3: Receiver operating characteristic curves of combined MR imaging–MR spectroscopic imaging values for individual readers.

Our study had a number of limitations. Like investigators in many other prostate MR studies, we used surgical histopathologic analysis as the reference standard. However, using this method, which superficially seems to be the most objective and scientific, has several consequences that may restrict the true benefits of imaging. As noted earlier, including only those patients who undergo surgery introduces a large selection bias because patients with high-risk disease are more likely to select nonsurgical treatment (37). Furthermore, the emphasis on comparing imaging analysis with histopathologic evaluation of tumor extent or stage ignores the issue that really matters to patients: the clinical outcome. It is conceivable that two tumors with the same histopathologic appearance can have quite different MR or MR spectroscopic imaging findings that are predictive of outcome. Such differences, which might be critical for improving specific clinical management and tailoring the adjuvant therapy to those at highest risk of recurrence, would be missed at histopathologic analysis. It is possible that future

prostate MR imaging–MR spectroscopic imaging trials will yield more favorable results if patients who are not undergoing surgery (particularly those who choose radiation therapy) are recruited and outcome, such as prostate-specific antigen level or survival, is used as the endpoint. There are disadvantages to using such an approach: 5–10 years of follow-up will be required to obtain meaningful endpoint data, and several confounders are likely to result from the differences in patient clinical management.

We did not analyze tumor stage as an endpoint in this study. This was a deliberate decision because prior study results indicate that the main benefit of using MR spectroscopic imaging is improved assessment of tumor volume, tumor aggressiveness, and tissue characterization, with an, at best, indirect benefit to staging accuracy (14,15,17,31,32). Furthermore, the importance of detecting extracapsular extension has recently been challenged owing to the reported good long-term outcomes after radical prostatectomy in men with extracapsular disease (38). Finally, accurate determination of the tumor location and the number of sextants involved seems to be becoming an increasingly important endpoint because of the recognition that tumor volume is an important prognostic indicator and the emergence of local therapies for prostate cancer (39,40).

In our study, we analyzed cancer in only the PZ, where most cancers occur. The morphologic and metabolic characteristics of central gland cancer at MR imaging and MR spectroscopic imaging are not as well established as those of PZ cancer (41–43), and imaging evaluation of the central part of the gland is complicated by the frequent coexistent heterogeneity introduced by benign prostatic hyperplasia. The finding that only 12 (11%) of the 108 patients with confirmed cancer at radical prostatectomy had isolated or dominant central gland tumor (as determined by the study pathologist) supports our decision to focus on PZ cancer. However, the lack of analysis of the central part of the gland was unquestionably a limitation of this study.

Another limitation was the manner in which the histopathologic and MR imaging data were correlated. In our opinion, using whole-mount sections to correlate MR imaging and histopathologic data is more precise than using standard blocks; however, we prepared only 20% of the radical prostatectomy tissue specimens by using whole-mount sections. Matching imaging and histopathologic data can be challenging, even with use of whole-mount sections, but it can be facilitated by acquiring the imaging data in the same plane as the histopathologic slices. Because this was not done in the current study, some of the histopathologic and imaging data correlations may have been unreliable; however, there is no reason to believe that the overall findings of this study were compromised.

Twenty-four of the 134 initially recruited patients were deemed ineligible. In a study such as this, with exacting and demanding inclusion criteria, this was not unexpected, and there is no reason to believe that any selection bias was introduced. Nevertheless, of the 24 ineligible patients, six were unable to complete the MR examination owing to anxiety or claustrophobia and one declined to undergo MR imaging after initial enrollment; these cases demonstrate that there may be a sizeable number of patients who do not willingly undergo MR imaging. Perhaps greater attention to patient comfort, increased use of sedation, and/or the use of wider or more open magnet bores could have alleviated this problem.

We did not use specific metabolic ratios as criteria for malignancy in this study, and some may consider this a limitation of the study design. Although the inclusion of metabolic ratios in previous scientific reports was appropriately objective, it may have created the perception that the interpretation of MR spectroscopic imaging data is largely quantitative. In reality, the day-to-day clinical interpretations of MR spectra are more complex. Automatically generated ratios are often meaningless because of noise (eg, negative numbers or values that are implausibly high or low), although visual evaluation of the spectra still may be possible. The spectra are not reviewed in isolation but rather in the context of the adjacent voxels. A voxel with an equivocally elevated choline concentration may be more or less suspicious depending on the choline level in the neighboring voxels. In practice, a voxel can be interpreted only after the corresponding T2-weighted images have been inspected to confirm that the tissue is predominantly prostatic and not contaminated by choline in the adjacent muscle or seminal vesicle. Knowledge of the T2-weighted image findings also might have a conscious or subconscious influence on one's spectroscopic data assessment. Such qualitative interpretation has been shown to have high accuracy in the differentiation of benign and malignant prostate tissue, with high interobserver agreement (31,44). Given these considerations, we opted to use a qualitative approach in this study.

Finally, this study should be viewed as a "snapshot" of the status of prostate MR imaging technology and experience during the period in which the described MR examinations were conducted—from 2004 to 2005. MR assessment of prostate cancer is rapidly evolving owing to the emergence of 3-T imagers (with high field strength facilitating greatly improved MR spectral quality and resolution), diffusion MR imaging, and dynamic contrast material–enhanced (perfusion) MR imaging (31,44–46). All of these techniques hold promise for facilitating improved prostate cancer imaging, and the role of the next multi-institutional study of endorectal MR imaging of prostate cancer may be to establish the relative benefit of using these different technologies at high field strength as part of a combined multiparametric examination.

Prostate cancer—involving both an organ and disease that are difficult to image—poses huge challenges for radiologists. However, the need for improved noninvasive risk-based stratification of patients with prostate cancer is great, and the modest results of our study should serve as an impetus to pursue novel and advanced diagnostic approaches rather than as an indicator that MR imaging has little to offer. The technical and logistic challenges that

were overcome and the experience gained in this study should be useful for future multi-institutional trials.

In conclusion, in patients with relatively low-volume and low-risk disease who undergo radical prostatectomy, the accuracy of combined endorectal MR imaging–MR spectroscopic imaging at 1.5 T for sextant localization of PZ prostate cancer is equal to that of MR imaging alone.

Acknowledgments: Medrad supplied the endorectal coils used in this study, and GE Healthcare provided technical support and the software used in this study.

References

1. American Cancer Society. Cancer facts and figures 2007. Publication no. 500807. Atlanta, Ga: American Cancer Society, 2006.
2. Brown ML, Lipscomb J, Snyder C. The burden of illness of cancer: economic cost and quality of life. Annu Rev Public Health 2001; 22:91–113.
3. Brown ML, Riley GF, Schussler N, Etzioni R. Estimated health care costs related to cancer treatment from SEER-Medicare data. Med Care 2002;40(8 suppl):IV–117.
4. Sakr WA, Grignon DJ. Prostate cancer: indicators of aggressiveness. Eur Urol 1997; 32(suppl 3):15–23.
5. Obek C, Louis P, Civantos F, Soloway MS. Comparison of digital rectal examination and biopsy results with the radical prostatectomy specimen. J Urol 1999;161:494–498.
6. Mettlin CJ, Black B, Lee F, et al. Workgroup #2: screening and detection—reference range/clinical issues of PSA. Cancer 1993; 71:2679–2680.
7. Salomon L, Colombel M, Patard JJ, et al. Value of ultrasound-guided systematic sextant biopsies in prostate tumor mapping. Eur Urol 1999;35:289–293.
8. Smith JA, Scardino PT, Resnick MI, et al. Transrectal ultrasound versus digital rectal examination for the staging of carcinoma of the prostate: results of a prospective multi-institutional trial. J Urol 1997;157:902–906.
9. Partin AW, Kattan MW, Subong EN, et al. Combination of prostate-specific antigen, clinical stage, and Gleason score to predict pathological stage of localized prostate cancer: a multi-institutional update. JAMA 1997;277: 1445–1451.
10. Partin AW, Mangold LA, Lamm DM, et al. Contemporary update of prostate cancer staging nomograms (Partin tables) for the new millennium. Urology 2001;58:843–848.
11. Huch Boni RA, Boner JA, Debatin JF, et al. Optimization of prostate carcinoma staging: comparison of imaging and clinical methods. Clin Radiol 1995;50:593–600.
12. Yu KK, Hricak H, Alagappan R, et al. Detection of extracapsular extension of prostate carcinoma with endorectal and phased-array coil MR imaging: multivariate feature analysis. Radiology 1997;202:697–702.
13. Kurhanewicz J, Vigneron DB, Hricak H, et al. Three-dimensional H-1 MR spectroscopic imaging of the in situ human prostate with high (0.24–0.7-cm^3) spatial resolution. Radiology 1996;198:795–805.
14. Scheidler J, Hricak H, Vigneron DB, et al. Prostate cancer: localization with three-dimensional proton MR spectroscopic imaging—clinicopathologic study. Radiology 1999; 213:473–480.
15. Coakley FV, Kurhanewicz J, Lu Y, et al. Prostate cancer tumor volume: measurement with endorectal MR and MR spectroscopic imaging. Radiology 2002;223:91–97.
16. Thornbury JR, Ornstein DK, Choyke PL, Langlotz CP, Weinreb JC. Prostate cancer: what is the future role for imaging? AJR Am J Roentgenol 2001;176:17–22.
17. Yu KK, Scheidler J, Hricak H, et al. Prostate cancer: prediction of extracapsular extension with endorectal MR imaging and three-dimensional proton MR spectroscopic imaging. Radiology 1999;213:481–488.
18. Kurhanewicz J, Vigneron DB, Hricak H, et al. Prostate cancer: metabolic response to cryosurgery as detected with 3D H-1 MR spectroscopic imaging. Radiology 1996;200: 489–496.
19. Schricker AA, Pauly JM, Kurhanewicz J, Swanson MG, Vigneron DB. Dualband spectral-spatial RF pulses for prostate MR spectroscopic imaging. Magn Reson Med 2001; 46:1079–1087.
20. Tran TK, Vigneron DB, Sailasuta N, et al. Very selective suppression pulses for clinical MRSI studies of brain and prostate cancer. Magn Reson Med 2000;43:23–33.
21. Wheeler TM, Lebovitz RM. Fresh tissue harvest for research from prostatectomy specimens. Prostate 1994;25:274–279.
22. American Joint Committee on Cancer. Prostate. In: Greene FL, Page DL, Fleming ID, et al, eds. AJCC cancer staging manual. 6th ed. New York, NY: Springer, 2002; 309–316.
23. Jung JA, Coakley FV, Vigneron DB, et al. Prostate depiction at endorectal MR spectroscopic imaging: investigation of a standardized evaluation system. Radiology 2004;233: 701–708.
24. Obuchowski NA. Nonparametric analysis of clustered ROC curve data. Biometrics 1997; 53:567–578.
25. Obuchowski NA. Multireader, multimodality receiver operating characteristic curve studies: hypothesis testing and sample size estimation using an analysis of variance approach with dependent observations. Acad Radiol 1995;2(suppl 1):S22–S29.
26. Obuchowski NA. Computing sample size for receiver operating characteristic studies. Invest Radiol 1994;29:238–243.
27. Obuchowski NA, McClish DK. Sample size determination for diagnostic accuracy studies involving binormal ROC curve indices. Stat Med 1997;16:1529–1542.
28. Obuchowski NA. Sample size calculations in studies of test accuracy. Stat Methods Med Res 1998;7:371–392.
29. Sadek AG, Mitchell DG, Siegelman ES, Outwater EK, Matteucci T, Hann HW. Early hepatocellular carcinoma that develops within macroregenerative nodules: growth rate depicted at serial MR imaging. Radiology 1995;195:753–756.
30. Hom JJ, Coakley FV, Simko JP, et al. Prostate cancer: endorectal MR imaging and MR spectroscopic imaging—distinction of true-positive results from chance-detected lesions. Radiology 2006;238:192–199.
31. Futterer JJ, Heijmink SW, Scheenen TW, et al. Prostate cancer localization with dynamic contrast-enhanced MR imaging and proton MR spectroscopic imaging. Radiology 2006;241:449–458.
32. Westphalen AC, Coakley FV, Qayyum A, et al. Peripheral zone prostate cancer: accuracy of different interpretative approaches with MR and MR spectroscopic imaging. Radiology 2008;246:177–184.
33. Testa C, Schiavina R, Lodi R, et al. Prostate cancer: sextant localization with MR imaging, MR spectroscopy, and ^{11}C-choline PET/CT. Radiology 2007;244:797–806.
34. Rifkin MD, Zerhouni EA, Gatsonis CA, et al. Comparison of magnetic resonance imaging and ultrasonography in staging early prostate cancer: results of a multi-institutional cooperative trial. N Engl J Med 1990;323: 621–626.
35. Tempany CM, Zhou X, Zerhouni EA, et al. Staging of prostate cancer: results of Radiology Diagnostic Oncology Group project comparison of three MR imaging techniques. Radiology 1994;192:47–54.
36. D'Amico AV, Whittington R, Malkowicz B, et al. Endorectal magnetic resonance imaging as a predictor of biochemical outcome after radical prostatectomy in men with clin-

ically localized prostate cancer. J Urol 2000; 164(3 pt 1):759–763.

37. Cooperberg MR, Grossfeld GD, Lubeck DP, Carroll PR. National practice patterns and time trends in androgen ablation for localized prostate cancer. J Natl Cancer Inst 2003;95:981–989.

38. Freedland SJ, Partin AW, Humphreys EB, Mangold LA, Walsh PC. Radical prostatectomy for clinical stage T3a disease. Cancer 2007;109:1273–1278.

39. Stamey TA, McNeal JE, Yemoto CM, Sigal BM, Johnstone IM. Biological determinants of cancer progression in men with prostate cancer. JAMA 1999;281:1395–1400.

40. Carroll PR, Presti JC Jr, Small E, Roach M 3rd. Focal therapy for prostate cancer 1996: maximizing outcome. Urology 1997;49(3a suppl):84–94.

41. Li H, Sugimura K, Kaji Y, et al. Conventional MRI capabilities in the diagnosis of prostate cancer in the transition zone. AJR Am J Roentgenol 2006;186:729–742.

42. Zakian KL, Eberhardt S, Hricak H, et al. Transition zone prostate cancer: metabolic characteristics at 1H MR spectroscopic imaging—initial results. Radiology 2003;229: 241–247.

43. Akin O, Sala E, Moskowitz CS, et al. Transition zone prostate cancers: features, detection, localization, and staging at endorectal MR imaging. Radiology 2006;239: 784–792.

44. Futterer JJ, Scheenen TW, Huisman HJ, et al. Initial experience of 3 tesla endorectal coil magnetic resonance imaging and 1H-spectroscopic imaging of the prostate. Invest Radiol 2004;39:671–680.

45. Futterer JJ, Engelbrecht MR, Huisman HJ, et al. Staging prostate cancer with dynamic contrast-enhanced endorectal MR imaging prior to radical prostatectomy: experienced versus less experienced readers. Radiology 2005;237:541–549.

46. Kozlowski P, Chang SD, Jones EC, et al. Combined diffusion-weighted and dynamic contrast-enhanced MRI for prostate cancer diagnosis: correlation with biopsy and histopathology. J Magn Reson Imaging 2006;24: 108–113.

Radiology 2009

This is your reprint order form or pro forma invoice

(Please keep a copy of this document for your records.)

Reprint order forms and purchase orders or prepayments must be received 72 hours after receipt of form either by mail or by fax at 410-820-9765. It is the policy of Cadmus Reprints to issue one invoice per order. **Please print clearly**.

Author Name _____
Title of Article _____
Issue of Journal_____ Reprint # _____ Publication Date _____
Number of Pages_____ KB # _____ Symbol Radiology
Color in Article? Yes / No (Please Circle)

Please include the journal name and reprint number or manuscript number on your purchase order or other correspondence.

Order and Shipping Information

Reprint Costs **(Please see page 2 of 2 for reprint costs/fees.)**

_____ Number of reprints ordered $_____
_____ Number of color reprints ordered $_____
_____ Number of covers ordered $_____
Subtotal $_____
Taxes $_____

(*Add appropriate sales tax for Virginia, Maryland, Pennsylvania, and the District of Columbia or Canadian GST to the reprints if your order is to be shipped to these locations*.)

First address included, add $32 for each additional shipping address $_____

TOTAL $_____

Shipping Address **(cannot ship to a P.O. Box) Please Print Clearly**

Name _____
Institution _____
Street _____
City _____ State _____ Zip _____
Country _____
Quantity_____ Fax _____
Phone: Day _____ Evening _____
E-mail Address _____

Additional Shipping Address* **(cannot ship to a P.O. Box)**

Name _____
Institution _____
Street _____
City _____ State _____ Zip _____
Country _____
Quantity _____ Fax _____
Phone: Day _____ Evening _____
E-mail Address _____

** Add $32 for each additional shipping address*

Payment and Credit Card Details

Enclosed: Personal Check _____
Credit Card Payment Details _____

Checks must be paid in U.S. dollars and drawn on a U.S. Bank.

Credit Card: __ VISA __ Am. Exp. __ MasterCard
Card Number _____
Expiration Date_____
Signature: _____

Please send your order form and prepayment made payable to:

Cadmus Reprints
P.O. Box 751903
Charlotte, NC 28275-1903

Note: Do not send express packages to this location, PO Box.

FEIN #:541274108

Invoice or Credit Card Information

Invoice Address **Please Print Clearly**

Please complete Invoice address as it appears on credit card statement

Name _____
Institution _____
Department _____
Street _____
City _____ State _____ Zip _____
Country _____
Phone _____ Fax _____
E-mail Address _____

Cadmus will process credit cards and *Cadmus Journal Services* will appear on the credit card statement.

If you don't mail your order form, you may fax it to 410-820-9765 with your credit card information.

Signature _____ Date _____

Signature is required. By signing this form, the author agrees to accept the responsibility for the payment of reprints and/or all charges described in this document.

RB-1/01/09

Radiology 2009

Black and White Reprint Prices

Domestic (USA only)						
# of Pages	50	100	200	300	400	500
1-4	$239	$260	$285	$303	$323	$340
5-8	$379	$420	$455	$491	$534	$572
9-12	$507	$560	$651	$684	$748	$814
13-16	$627	$698	$784	$868	$954	$1,038
17-20	$755	$845	$947	$1,064	$1,166	$1,272
21-24	$878	$985	$1,115	$1,250	$1,377	$1,518
25-28	$1,003	$1,136	$1,294	$1,446	$1,607	$1,757
29-32	$1,128	$1,281	$1,459	$1,632	$1,819	$2,002
Covers	$149	$164	$219	$275	$335	$393

International (includes Canada and Mexico)						
# of Pages	50	100	200	300	400	500
1-4	$299	$314	$367	$429	$484	$546
5-8	$470	$502	$616	$722	$838	$949
9-12	$637	$687	$852	$1,031	$1,190	$1,369
13-16	$794	$861	$1,088	$1,313	$1,540	$1,765
17-20	$963	$1,051	$1,324	$1,619	$1,892	$2,168
21-24	$1,114	$1,222	$1,560	$1,906	$2,244	$2,588
25-28	$1,287	$1,412	$1,801	$2,198	$2,607	$2,998
29-32	$1,441	$1,586	$2,045	$2,499	$2,959	$3,418
Covers	$211	$224	$324	$444	$558	$672

Color Reprint Prices

Domestic (USA only)						
# of Pages	50	100	200	300	400	500
1-4	$247	$267	$385	$515	$650	$780
5-8	$297	$435	$655	$923	$1194	$1467
9-12	$445	$563	$926	$1,339	$1,748	$2,162
13-16	$587	$710	$1,201	$1,748	$2,297	$2,843
17-20	$738	$858	$1,474	$2,167	$2,846	$3,532
21-24	$888	$1,005	$1,750	$2,575	$3,400	$4,230
25-28	$1,035	$1,164	$2,034	$2,986	$3,957	$4,912
29-32	$1,186	$1,311	$2,302	$3,402	$4,509	$5,612
Covers	$149	$164	$219	$275	$335	$393

International (includes Canada and Mexico))						
# of Pages	50	100	200	300	400	500
1-4	$306	$321	$467	$642	$811	$986
5-8	$387	$517	$816	$1,154	$1,498	$1,844
9-12	$574	$689	$1,157	$1,686	$2,190	$2,717
13-16	$754	$874	$1,506	$2,193	$2,883	$3,570
17-20	$710	$1,063	$1,852	$2,722	$3,572	$4,428
21-24	$1,124	$1,242	$2,195	$3,231	$4,267	$5,300
25-28	$1,320	$1,440	$2,541	$3,738	$4,957	$6,153
29-32	$1,498	$1,616	$2,888	$4,269	$5,649	$7028
Covers	$211	$224	$324	$444	$558	$672

Minimum order is 50 copies. For orders larger than 500 copies, please consult Cadmus Reprints at 800-407-9190.

Reprint Cover

Cover prices are listed above. The cover will include the publication title, article title, and author name in black.

Shipping

Shipping costs are included in the reprint prices. Domestic orders are shipped via FedEx Ground service. Foreign orders are shipped via a proof of delivery air service.

Multiple Shipments

Orders can be shipped to more than one location. Please be aware that it will cost $32 for each additional location.

Delivery

Your order will be shipped within 2 weeks of the journal print date. Allow extra time for delivery.

Tax Due

Residents of Virginia, Maryland, Pennsylvania, and the District of Columbia are required to add the appropriate sales tax to each reprint order. For orders shipped to Canada, please add 7% Canadian GST unless exemption is claimed.

Ordering

Reprint order forms and purchase order or prepayment is required to process your order. Please reference journal name and reprint number or manuscript number on any correspondence. You may use the reverse side of this form as a proforma invoice. Please return your order form and prepayment to:

Cadmus Reprints
P.O. Box 751903
Charlotte, NC 28275-1903

Note: Do not send express packages to this location, PO Box.
FEIN #:541274108

Please direct all inquiries to:

Rose A. Baynard
800-407-9190 (toll free number)
410-819-3966 (direct number)
410-820-9765 (FAX number)
baynardr@cadmus.com (e-mail)

Reprint Order Forms and purchase order or prepayments must be received 72 hours after receipt of form.